Weak- and hyperfine-interaction-induced 1s2s $^1S_0 \rightarrow 1s^2\ ^1S_0$ E1 transition rates of He-like ions*

Laima Radžiūtė[a], Erikas Gaidamauskas[a], Gediminas Gaigalas[a]†, Li Ji-Guang(李冀光)[b]‡, Dong Chen-Zhong(董晨钟)[c], and Per Jönsson[d]

[a] *Vilnius University, Institute of Theoretical Physics and Astronomy, A. Goštauto* 12, *LT*-01108, *Vilnius, Lithuania*

[b] *Data Center for High Energy Density Physics, Institute of Applied Physics and Computational Mathematics, Beijing* 100088, *China*

[c] *Key Laboratory of Atomic and Molecular Physics and Functional Materials of Gansu Province, College of Physics and Electronic Engineering, Northwest Normal University, Lanzhou* 730070, *China*

[d] *Materials Science and Applied Mathematics, Malmö University, S*-20506 *Malmö, Sweden*

(Received 6 August 2014; revised manuscript received 28 November 2014; published online 10 February 2015)

Weak- and hyperfine-interaction-induced 1s2s $^1S_0 \rightarrow 1s^2\ ^1S_0$ E1 transition rates for the isoelectronic sequence of He-like ions have been calculated using the multiconfiguration Dirac–Hartree–Fock (MCDHF) and relativistic configuration interaction methods. The results should be helpful for the future experimental investigations of parity non-conservation effects.

Keywords: parity non-conservation effect, hyperfine interaction, MCDHF method

PACS: 31.30.Gs, 31.15.V−, 31.15.ag, 11.30.Er **DOI:** 10.1088/1674-1056/24/4/043103

1. Introduction

Weak interaction effects in atomic physics play a very important role in searching for a new physics beyond the standard model of elementary particles. There are a number of experimental and theoretical investigations of the parity-violation effects in heavy neutral atoms.[1,2] However, correlation effects are the main source of uncertainty in theoretical results. Therefore, it looks promising to investigate relatively simple highly charged few-electrons ions in order to minimize the impact of correlation effects.

Gorshkov and Labzovskiĭ[3] and Labzowsky *et al.*[4] have proposed that the mixed hyperfine and weak-quenching can be used to test parity-violation effects. The one-photon transition 1s2s $^1S_0 \rightarrow 1s^2\ ^1S_0$ of He-like ions is considered as a good candidate for these tests and the relvent experiments will be carried out at GSI.[5] The transition is due to several competing processes (see Fig. 1). In the first process the 1s2s $^1S_0$ state is mixed with 1s2p $^3P_0$ due to the weak interaction between the electrons and the nucleus. The 1s2p $^3P_0$ state, in turn, is mixed with 1s2p $^3P_1$ and 1s2p $^1P_1$ due to the off-diagonal hyperfine interaction opening the 1s2s $^1S_0 \rightarrow 1s^2\ ^1S_0$ E1 transition. In the second process the 1s2s $^1S_0$ and 1s2s $^3S_1$ states are mixed due to the off-diagonal hyperfine interaction opening the 1s2s $^1S_0 \rightarrow 1s^2\ ^1S_0$ M1 transition. The latter transition has recently been studied by Li *et al.*[6] The third and the dominant 1s2s $^1S_0 \rightarrow 1s^2\ ^1S_0$ decay channel is the two-photon 2E1 transition. Relevant data for the combined weak- and hyperfine interaction-induced 1s2s $^1S_0 \rightarrow 1s^2\ ^1S_0$ E1 transition are however still insufficient and in response to this we have performed systematic calculations along the He-like iso-electronic sequence using the relativistic atomic structure package GRASP2K.

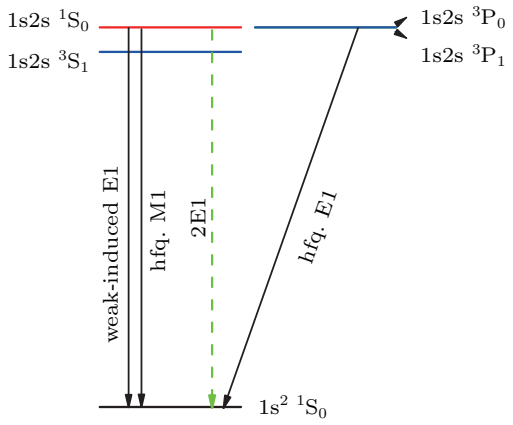

Fig. 1. Energy level and transition scheme for He-like ion. hfq. E1 represents hyperfine E1 electrical dipole-induced transition, hfq. M1 hyperfine M1 magnetic dipole-induced transition, and weak-incuced weak- and hyperfine-induced E1 electrical dipole transition, 2E1 two-photon electric dipole transition.

2. Theory

In the multiconfiguration Dirac–Hartree–Fock (MCDHF) method, the atomic state function (ASF) $\Psi(\gamma PJM_J)$ of a stationary state of an atom is expressed as a linear combination of symmetry-adapted configuration state functions (CSFs)

*Project supported by the National Natural Science Foundation of China (Grant Nos. 11274254, 11147108, U1331122, and U1332206), in part by the National Basic Research Program of China (Grant No. 2013CB922200), and the National Natural Science Foundation of China (Grant No. 10979007).

†Corresponding author. E-mail: gediminas.gaigalas@tfai.vu.lt

‡Corresponding author. E-mail: Li_Jiguang@iapcm.ac.cn

$\Phi(\gamma_p PJM_J)$, i.e.

$$\Psi(\gamma PJM_J) = \sum_p c_p \Phi(\gamma_p PJM_J), \tag{1}$$

where J is the total electronic angular momentum of the state, γ represents the electronic configuration and intermediate quantum numbers whereas P stands for the parity. The mixing coefficients c_p and the one-electron radial wave functions, building the CSFs, are obtained in a self-consistent procedure by optimization of the energy functional based on the Dirac–Coulomb Hamiltonian (in atomic unit: a.u.)

$$H_{\rm DC} = \sum_{j=1}^{N} \Big(c\boldsymbol{\alpha}_j \cdot \boldsymbol{p}_j + (\beta_j - 1)c^2 + V(r_j) \Big) + \sum_{j<k}^{N} \frac{1}{r_{jk}}, \tag{2}$$

where $V(r_j)$ is the monopole part of the electron–nucleus interaction.[7,8] The nuclear charge distribution is modeled by a two-component Fermi distribution. The MCDHF calculations were performed with the GRASP2K relativistic atomic structure package.[9,10] In calculations of spin-angular parts of matrix elements the second quantization method in coupled tensorial form and the quasispin technique[11] were adopted.

In relativistic calculations the ASFs are given in jj-coupling. To adhere to the labeling conventions used by the experimentalists, the ASFs are transformed from jj-coupling to LS-coupling using the methods developed in Refs. [12] and [13]. The relativistic configuration interaction (RCI) method was also used to include the transverse Breit interaction and QED corrections: self-energy and vacuum polarization. The details of these corrections are discussed in Ref. [8]. In the presence of hyperfine interaction the coupled wave function of total system of the electrons and the nucleus can be written as

$$\begin{aligned}\Psi(\gamma\nu PJIFM_F) = & \sum_{M_J M_I} \langle JIM_J M_I | JIFM_F \rangle \\ & \times \Psi(\gamma PJM_J)\Psi(\nu IM_I), \end{aligned} \tag{3}$$

where the expansion coefficients are the Clebsch–Gordan coefficients, I is the nuclear spin, F is the total angular momentum of the combined system. The wave function $\Psi(\nu IM_I)$ corresponds to the ground state of the nucleus. Taking the off-diagonal part of the hyperfine interaction into account the total wave function of an atom can be expressed as

$$\begin{aligned}\Psi(\gamma\nu PIFM_F) = & \, a_0 \Psi(\gamma\nu PJIFM_F) \\ & + \sum_{l=1}^{n} a_l \Psi(\alpha_l \nu PJ_l IFM_F). \end{aligned} \tag{4}$$

The off-diagonal hyperfine interaction is quite weak and the coefficient a_0 of the dominant function can be set to 1 and expansion coefficients can be perturbatively approximated as

$$a_l = \frac{\langle \Psi(\alpha_l \nu PJ_l IFM_F) | H_{\rm hfs} | \Psi(\gamma\nu PJIFM_F) \rangle}{E(\gamma PJ) - E(\alpha_l PJ_l)}, \tag{5}$$

where $H_{\rm hfs}$ is the hyperfine interaction operator.[14] In this work we only include the nuclear magnetic dipole hyperfine interaction.

Due to the parity-violating exchange of neutral Z^0 bosons between the electrons and nucleus, all atomic states are mixed with states of opposite parity. Spin-independent parity-nonconservating weak interaction between the electrons and nucleus is given by (in atomic unit: a.u.)[1,2]

$$H_{\rm W} = \frac{G_{\rm F}}{2\sqrt{2}} Q_{\rm W} \sum_{j=1}^{N} \gamma_j^5 \rho(r_j), \tag{6}$$

where $G_{\rm F}$ is the Fermi constant, $Q_{\rm W} = Z(1 - 4\sin^2\Theta_{\rm W}) - N$ the weak charge of the nucleus, γ^5 the Dirac matrix, and $\rho(r)$ the normalized (to unity) Fermi nuclear density function. In our calculations we put $\sin^2\Theta_{\rm W} = 0.2312$ for the Weinberg angle $\Theta_{\rm W}$.[15] This interaction mixes parity of atomic states and also opens new decay channels. The total atomic wave function with mixed parity can be expressed as:

$$\begin{aligned}\widetilde{\Psi}(\gamma\nu IFM_{\rm F}) = & \, b_0 \Psi(\gamma\nu PIFM_{\rm F}) \\ & + \sum_{r=1}^{m} b_r \Psi(\alpha_r \nu(-P)IFM_{\rm F}). \end{aligned} \tag{7}$$

The parity non-conserving interaction, like the off-diagonal hyperfine interaction, is quite weak and the coefficient b_0 of the dominant function can be set to 1 and expansion coefficients can also be perturbatively approximated as:

$$b_r = \frac{\langle \Psi(\alpha_r(-P)J_r M_{J_r}) | H_{\rm W} | \Psi(\gamma PJM_J) \rangle}{E(\gamma PJ) - E(\alpha_r(-P)J_r)}. \tag{8}$$

The rate of the spontaneous one-photon electric dipole (E1) transition between two atomic states with mixed parity is given by (in atomic unit a.u.):[16,17]

$$A = \frac{4\omega^3}{3c^3} \sum_{M_{\rm F},q} \left| \langle \widetilde{\Psi}(\gamma\nu IFM_{\rm F}) | Q_q^1 | \widetilde{\Psi}(\gamma'\nu IF'M'_{\rm F}) \rangle \right|^2, \tag{9}$$

where Q^1 is the operator of the electric dipole transitions. Substituting Eqs. (4) and (7) into expression (9) and summing over the projections of the angular momenta gives

$$\begin{aligned} A = & \frac{4\omega^3}{3c^3} \frac{1}{2F'+1} \\ & \times \left| \sum_{l,r,l',r'} a_l^* a'_l b_r^* b_{r'} \langle \Psi(\gamma_{lr}\nu P_r J_l IF) || Q^1 || \Psi(\gamma_{l'r'}\nu P_{r'} J_{l'} IF') \rangle \right|^2. \end{aligned} \tag{10}$$

This expression can also be written (in unit s^{-1}) as:

$$\begin{aligned} A = & \frac{2.02613 \times 10^{18}}{\lambda^3} \frac{1}{2F'+1} \\ & \times \left| \sum_{l,r,l',r'} a_l^* a'_l b_r^* b_{r'} \langle \Psi(\gamma_{lr}\nu P_r J_l IF) || Q^1 || \Psi(\gamma_{l'r'}\nu P_{r'} J_{l'} IF') \rangle \right|^2, \end{aligned} \tag{11}$$

where λ is the wavelength in unit Å for the transition. This perturbative formalism does not include the radiation-damping

effects, which are important when radiative line width is comparable to the separation between fine structure levels.[18]

The reduced matrix (submatrix) element of the electric dipole transition operator can be expressed as

$$\begin{aligned}&\langle\Psi(\gamma_{l_r}\nu P_r J_l IF)\,||Q^1||\Psi(\gamma_{l'_{r'}}\nu P_{r'} J_{l'} IF')\rangle\\&=(-1)^{I+J_l+F'+1}\delta(P_r,-P_{r'})\sqrt{(2F+1)(2F'+1)}\\&\quad\times\begin{Bmatrix}J & F & I\\ F' & J_{l'} & 1\end{Bmatrix}\langle\Psi(\gamma_{l_r}P_r J_l)\,\|Q^1\|\Psi(\gamma_{l'_{r'}}(-P_r)J_{l'})\rangle.\end{aligned}\quad(12)$$

The square of the absolute value of last reduced matrix element is the line strength. Applying Wigner–Eckart theorem, the matrix element of the weak interaction operator can be expressed as

$$\begin{aligned}&\langle\Psi(\gamma PJM_J)\,|H_{\rm W}|\Psi(\gamma'(-P)J'M'_J)\rangle\\&=\delta(J,J')\delta(M_J,M'_J)\left[\Psi(\gamma PJ)\,\|H_{\rm W}\|\Psi(\gamma'(-P)J')\right],\end{aligned}\quad(13)$$

where $\langle\gamma'J'\|H_{\rm W}\|\gamma J\rangle=\sqrt{2J'+1}[\gamma'J'\|H_{\rm W}\|\gamma J]$. Using multiconfiguration expansions the reduced matrix elements of the general spherical tensor operator T^k_q can be written as

$$\begin{aligned}&\left[\Psi(\gamma PJ)\,\|T^k\|\Psi(\gamma'(-P)J')\right]\\&=\sum_{p,s}c_pc_s\left[\Phi(\gamma_pPJ)\,\|T^k\|\Phi(\gamma_s(-P)J')\right].\end{aligned}\quad(14)$$

Reduced matrix elements of one-electron operator between configuration state functions can be expressed as sums over elements involving single-particle orbitals

$$\begin{aligned}&\left[\Phi(\gamma_pPJ)\|T^k\|\Phi(\gamma_s(-P)J')\right]\\&=\sum_{a,b}d^k_{ab}(ps)\left[n_a\kappa_a\|t^k\|n_b\kappa_b\right],\end{aligned}\quad(15)$$

where $d^k_{ab}(ps)$ are the spin-angular coefficients that arise from using Racah's algebra in the decomposition of the one-electron operator matrix element. The single-particle reduced matrix element can be factorized into a reduced angular matrix element and a radial integral. Here we give the factorization of the reduced matrix element of the weak interaction ($k=0$)

$$\begin{aligned}&[n_a\kappa_a\|h_W\|n_b\kappa_b]\\&=\delta(-\kappa_a,\kappa_b)\,{\rm i}\,\frac{G_{\rm F}}{2\sqrt{2}}Q_{\rm W}\int_0^\infty(P_bQ_a-P_aQ_b)\,\rho(r)\,{\rm d}r,\end{aligned}\quad(16)$$

where ${\rm i}=\sqrt{-1}$ is the imaginary unit. In the radial integral P and Q are the large and small components of the relativistic one-electron radial wave function. For the calculations of the matrix elements we extended the GRASP2K relativistic atomic structure package. The extension, presented in this work, includes programs for the weak interaction matrix elements.

3. Results and discussion

For the generation of the MCDHF expansion (1) we used the active space approach. The energy functional on which the orbitals were optimized is defined according to an extended optimal level (EOL) scheme, where a linear combination of the seven lowest atomic states is used. The combination includes two even states with $J=0$, one odd state with $J=0$, two odd states with $J=1$, one even state with $J=1$ and one odd state with $J=2$. CSFs are generated using active sets (AS) of orbitals. CSFs of the multiconfiguration calculations include single and double substitutions from the 1s shell. The AS is labeled by an integer n and includes s, p, d, f, and g orbitals up to n. For example, the active set $\mathrm{AS}_n=4$ contains s, p, d orbitals up to $n=4$ and 4f orbital. The active sets were extended to $n=6$ for $Z=6$–61 and to $n=5$ for $Z=62$–92 ions. At all steps only new orbitals are optimized. For example, in the first calculation for the active set (AS_2) all orbitals are optimized. In the next step the orbitals (1s 2s 2p) of AS_2 are frozen and only the new orbitals (3s 3p 3d) from the active set AS_3 are optimized.

Table 1 illustrates the convergence of the transition energies for the $^{13}_{6}$C and $^{149}_{62}$Sm ions (transverse Breit interaction is included). As can be see from the table correlation effects have a huge impact on the results for $^{13}_{6}$C, but the QED contribution to the total value is very small (22% for ΔE_2) compared with the much heavier $^{149}_{62}$Sm (3 226% for ΔE_2). QED affects mostly the ΔE_2 transition. As can be see from the table, results for $^{13}_{6}$C are in a good agreement with experiments.[21]

Table 1. Transition energies in cm^{-1} for ^{13}C and ^{149}Sm from calculations with increasing active sets including Breit interaction. $\Delta E_1 = E\left(1s^2\ {}^1S_0\right)-E\left(1s2s\ {}^1S_0\right)$, $\Delta E_2 = E\left(1s2s\ {}^1S_0\right)-E\left(1s2p\ {}^3P_0\right)$, and $\Delta E_3 = E\left(1s2p\ {}^3P_1\right)-E\left(1s2p\ {}^3P_0\right)$. QED corrections were calculated using active spaces of CSFs formed by the AS_4.

Active set	CSFs	ΔE_1	ΔE_2	ΔE_3	ΔE_1	ΔE_2	ΔE_3
		^{13}C			^{149}Sm		
AS_2	7	−2439452	4300.3	−12.707	−326570125	−70225.5	−125804
AS_3	67	−2453255	1073.2	−12.422	−326591828	−77716.2	−125123
AS_4	187	−2454485	194.3	−12.312	−326596149	−79759.3	−124974
AS_5	397	−2454842	−3.0	−12.730	−326597470	−80513.8	−124930
AS_6	697	−2455131	−107.8	−12.620	−326599124	−81059.4	−124898
QED correction	187	184	19.2	0.200	471383	83651.8	−105
Total value		−2454947	−88.6	−12.420	−326127741	2592.4	−125003
Ref. [19]		−2455167	−140.2	−12.488	−326137507	4973.3	−124809
Ref. [20]					−326136354	3645.0	−124910
Experiment[21]		−2455026	−144.4	−12.6			

Also it should be mentioned, that for ions with $Z = 14$, 26, 31, 37, 42, 45, 50, 54, 61–63, 91, and 92, Coulomb and Breit interactions give incorrect positions of excited levels (comparing with data in Refs. [19] and [20]) and only when QED are introduced is the order correct. For ions $Z = 6$, 64, 65, 71, 77, and 90 correct order of excited levels was obtained including the Breit interaction. Specific cases are ions with $Z = 9$ and 22. In the first case the energy levels are in the correct order when including the Coulomb interaction, but by adding the Breit interaction energies the order is incorrect. Including QED effect we again get the correct energy spectrum. In the second case the correct order was obtained by including the Coloumb interaction and the Breit interaction and QED does not influence the order.

We also calculated the line strengths of the $1s2p\ ^3P_1 \rightarrow 1s^2\ ^1S_0$ E1 transitions in the Coulomb gauge (Table 2):

$$S_{\mathrm{E1}} = \left|\langle \Psi\left(1s^2\ ^1S_0\right)||Q^1||\Psi\left(1s2p\ ^3P_1\right)\rangle\right|^2. \tag{17}$$

Line strengths are compared with data from Ref. [22] and the difference is at most 5.5%. This shows that wave functions are appropriate for weak and hyperfine interactions calculations.

Table 2. The wavelengths λ in unit Å for the $1s2s\ ^1S_0 \rightarrow 1s^2\ ^1S_0$ E1 transition and line strengths S_{E1} Eq. (19) in atomic unit a.u. for the $1s2p\ ^3P_1 \rightarrow 1s^2\ ^1S_0$ E1 transition of He-like ions.

	λ/Å		Line strength	
Isotope	This work	Ref. [19], [20]	S_{E1}	Ref. [22]
$^{13}_{6}$C	40.728	40.730[a)]	2.8909[−6]	2.8309[-6]
$^{19}_{9}$F	16.942	16.940[a)]	1.3343[−5]	1.3219[-5]
$^{29}_{14}$Si	6.6851	6.6850	6.9859[−5]	6.9556[-5]
$^{47}_{22}$Ti	2.6226	2.6225	2.9941[−4]	2.9855[-4]
$^{57}_{26}$Fe	1.8594	1.8584	4.2208[−4]	4.2092[-4]
$^{71}_{31}$Ga	1.2950	1.2949	5.0259[−4]	5.0116[-4]
$^{85}_{37}$Rb	0.8995	0.8995	4.9500[−4]	4.9352[-4]
$^{97}_{42}$Mo	0.6923	0.6923	4.4597[−4]	4.4446[-4]
$^{103}_{45}$Rh	0.6001	0.6001	4.1101[−4]	4.0950[-4]
$^{117}_{50}$Sn	0.4820	0.4820	3.5342[−4]	3.5177[-4]
$^{131}_{54}$Xe	0.4104	0.4104	3.1152[−4]	3.0961[-4]
$^{145}_{61}$Pm	0.3174	0.3174	2.4924[−4]	2.4696[-4]
$^{149}_{62}$Sm	0.3066	0.3066	2.4187[−4]	2.3915[-4]
$^{151}_{63}$Eu	0.2964	0.2964	2.3441[−4]	2.3160[-4]
$^{155}_{64}$Gd	0.2866	0.2866	2.2689[−4]	2.2431[-4]
$^{159}_{65}$Tb	0.2773	0.2773	2.2037[−4]	2.1727[-4]
$^{175}_{71}$Lu	0.2294	0.2293	1.8383[−4]	1.7984[-4]
$^{193}_{77}$Ir	0.1922	0.1922	1.5345[−4]	1.4942[-4]
$^{229}_{90}$Th	0.1355	0.1355	1.0620[−4]	1.0088[-4]
$^{231}_{91}$Pa	0.1321	0.1321	1.0333[−4]	9.7885[-5]
$^{235}_{92}$U	0.1288	0.1288	1.0016[−4]	9.4994[-5]

[a)] For the calculations of the wavelengths the values of the $E\left(1s2s\ ^1S_0\right)$ and $E\left(1s^2\ ^1S_0\right)$ were used from Ref. [19].

For the E1 transition $1s2s\ ^1S_0 \rightarrow 1s^2\ ^1S_0$, as mentioned above, the important mixing of $1s2p\ ^3P_0$ with $1s2p\ ^3P_1$ is due to off-diagonal hyperfine interaction and the mixing of $1s2s\ ^1S_0$ with $1s2p\ ^3P_0$ is due to the weak interaction. Mixing coefficients a_1 and b of these interactions are given by

$$a_1 = \frac{\langle \Psi\left(1s2p\ ^3P_1F\right)|H_{\mathrm{hfs}}|\Psi\left(1s2p\ ^3P_0F\right)\rangle}{E\left(1s2p\ ^3P_0\right) - E\left(1s2p\ ^3P_1\right)}, \tag{18}$$

$$b = \frac{\langle \Psi\left(1s2p\ ^3P_0\right)|H_{\mathrm{W}}|\Psi\left(1s2s\ ^1S_0\right)\rangle}{E\left(1s2s\ ^1S_0\right) - E\left(1s2p\ ^3P_0\right)}, \tag{19}$$

where $F = I$. The calculated off-diagonal hyperfine interaction matrix elements and corresponding mixing coefficients (a_1), using obtained atomic wave functions, are presented in Table 3. Transition energies in the expressions above are calculated including the Breit interaction and QED effects. For elements $^{13}_{6}$C, $^{19}_{9}$F, $^{29}_{14}$Si, $^{47}_{22}$Ti, and $^{155}_{64}$Gd a_1 values were calculated by the direct diagonalization of the full atomic hamiltonian and are given in the brackets. The differences between these hyperfine mixing coefficients and coefficients calculated with Eq. (18) are less than 1% and support the applicability of the perturbative expression. It should be mentioned that QED does not affect the ΔE_3 transition energy (up to 0.9%) and the a_1 mixing coefficient. The magnitude of the mixing coefficients for the $^{151}_{63}$Eu and $^{155}_{64}$Gd ions are in agreement with values from Ref. [4] -4.24×10^{-2} and 3.35×10^{-3} respectively, there differences in a sign are due to the different definitions of the phase factor in the hyperfine interaction matrix element.

The calculated values of the weak interaction matrix element and corresponding mixing coefficients (b/i) are presented in Table 4. Due to the importance of the QED effects for the heavy ions,[23] transition energies are taken from accurate calculations by Plante *et al.*[19] and results of the Artemyev *et al.*[20] The first author included QED effect of order $(Z\alpha)^3$ and some terms of $(Z\alpha)^4$ and the second author evaluated terms complete through order $(Z\alpha)^4$.

Compared with Plante *et al.*[19] and Artemyev *et al.*[20] our calculated QED contributions to the ΔE_2 transition energies are too large. For example, QED contribution for $^{117}_{50}$Sn in our calculation is 0.2059 a.u. as compared to 0.1818 a.u.[19] and 0.1845 a.u.[20] (235%, 197%, and 206% of total transition energy respectively). Another example is $^{229}_{90}$Th. For the ΔE_2 transition energy the contribution from QED in our calculation is 1.8573 a.u. as compared to 1.4259 a.u.[19] and 1.4651 a.u.[20] For $^{151}_{63}$Eu the QED contribution is 15528% to the total ΔE_2 transition energy. This mean that QED effects not only change relative position of the levels, but also decrease transition energy and increase mixing coefficients of weak interaction (without QED $b/\mathrm{i} = -0.99347 \times 10^{-8}$).

The values for the $^{151}_{63}$Eu and $^{155}_{64}$Gd ions, 0.31767×10^{-6} and 0.85603×10^{-6} respectively, have been calculated with the same energies as those in Ref. [4] and [19]. Using these energies there is a good agreement with the values 0.33[−6] and 0.91[−6] given by Labzowsky.[4] This means that the calculated matrix element of the weak interaction is very close to the one computed by us.

Table 3. Off-diagonal hyperfine interaction matrix elements $\langle|h_{\rm hfs}|\rangle_1$ (in atomic unit a.u.) and mixing coefficients (a_1 and a_1') Eq. (17) due to the hyperfine interactions for He-like ions. For the calculations of a_1' the values of $E\left(1s2p\ ^3P_0\right)$ and $E\left(1s2p\ ^3P_1\right)$ were used from Refs. [19] and [20]. The values in the brackets were calculated by the direct diagonalization of the atomic Hamiltonian matrix.

				The mixing coefficients		
Isotope	I	μ_I	$\langle\|h_{\rm hfs}\|\rangle_1$	a_1	a_1'	Ref. [4]
$^{13}_{6}$C	1/2	0.7024	3.9931[−6]	0.68257[−1]	0.70176[−1][a)]	
					(0.69661[−1])	
$^{19}_{9}$F	1/2	2.6289	5.0943[−5]	−0.73246[−1]	−0.73905[−1][a)]	
					(−0.73308[−1])	
$^{29}_{14}$Si	1/2	−0.5553	−4.2065[−5]	0.51889[−2]	0.51959[−2]	
					(0.51957[−2])	
$^{47}_{22}$Ti	5/2	−0.7885	−1.7482[−4]	0.36554[−2]	0.36607[−2]	
					(0.36606[−2])	
$^{57}_{26}$Fe	1/2	0.0906	5.0963[−5]	−0.68638[−3]	−0.68734[−3]	
$^{71}_{31}$Ga	3/2	2.5623	1.9132[−3]	−0.19709[−1]	−0.19735[−1]	
$^{85}_{37}$Rb	5/2	1.3534	1.6521[−3]	−0.17996[−1]	−0.18021[−1]	
$^{97}_{42}$Mo	5/2	−0.9335	−1.7306[−3]	0.34071[−1]	0.34128[−1]	
$^{103}_{45}$Rh	1/2	−0.8840	−3.0208[−3]	0.39394	0.39577	
$^{117}_{50}$Sn	1/2	−1.0010	−4.8927[−3]	−0.49441[−1]	−0.49477[−1]	
$^{131}_{54}$Xe	3/2	0.6918	3.2932[−3]	0.15025[−1]	0.15037[−1]	
$^{145}_{61}$Pm	5/2	3.8000	2.5713[−2]	0.49751[−1]	0.49792[−1]	
$^{149}_{62}$Sm	7/2	−0.6677	−4.5978[−3]	−0.80723[−2]	−0.80787[−2]	
$^{151}_{63}$Eu	5/2	3.4717	2.6481[−2]	0.42363[−1]	0.42438[−1]	−0.424[−1]
$^{155}_{64}$Gd	3/2	−0.2572	−2.2708[−3]	−0.33223[−2]	−0.33247[−2]	0.335[−2]
					(−0.33246[−2])	
$^{159}_{65}$Tb	3/2	2.0140	1.8855[−2]	0.25311[−1]	0.25328[−1]	
$^{175}_{71}$Lu	7/2	2.2323	2.5881[−2]	0.21896[−1]	0.21913[−1]	
$^{193}_{77}$Ir	3/2	0.1637	3.0154[−3]	0.17182[−2]	0.17189[−2]	
$^{229}_{90}$Th	5/2	0.4600	1.5746[−2]	0.43361[−2]	0.43334[−2]	
$^{231}_{91}$Pa	3/2	2.0100	7.9272[−2]	0.20739[−1]	0.20721[−1]	
$^{235}_{92}$U	7/2	−0.3800	−1.3896[−2]	−0.34557[−2]	−0.34524[−2]	

[a)] For the calculations of the mixing coefficients the values of the $E\left(1s2p\ ^3P_0\right)$ and $E\left(1s2p\ ^3P_1\right)$ were used from Ref. [19].

Table 4. The matrix element of the weak interaction operator (in $\mathrm{i}\frac{G_{\rm F}}{2\sqrt{2}}Q_{\rm W}$ a.u.), mixing coefficients (b and b') Eq. (18) due to the weak interactions and transition rates A_1 Eq. (20) in unit s^{-1} of the weak and hyperfine-induced $1s2s\ ^1S_0 \to 1s^2\ ^1S_0$ E1 transitions for He-like ions. For calculation of b' and the values of $E\left(1s2s\ ^1S_0\right)$ and $E\left(1s2p\ ^3P_0\right)$ were used from Refs. [19] and [20].

		The mixing coefficients				
Isotope	$\langle\|W\|\rangle$	b/i	b'/i[19]	b'/i[20]	Ref. [4]	A_1
$^{13}_{6}$C	−1.0652[−1]	−0.79193[−11]	−0.72709[−11]			0.73669[−17][a)]
$^{19}_{9}$F	−6.4268[−1]	0.28717[−11]	0.31168[−11]			0.97443[−16][a)]
$^{29}_{14}$Si	−4.3718	0.10812[−10]	0.10838[−10]	0.10840[−10]		0.49881[−15]
$^{47}_{22}$Ti	−3.1642[1]	0.75766[−10]	0.75711[−10]	0.75772[−10]		0.86010[−12]
$^{57}_{26}$Fe	−6.7191[1]	0.16964[−9]	0.16915[−9]	0.16944[−9]		0.59978[−12]
$^{71}_{31}$Ga	−1.5201[2]	0.42552[−9]		0.42404[−9]		0.10916[−7]
$^{85}_{37}$Rb	−3.5815[2]	0.11571[−8]		0.11497[−8]		0.19659[−6]
$^{97}_{42}$Mo	−6.8249[2]	0.25753[−8]	0.25154[−8]	0.25463[−8]		0.68307[−5]
$^{103}_{45}$Rh	−9.8340[2]	0.41033[−8]		0.40403[−8]		0.32719[−2]
$^{117}_{50}$Sn	−1.7559[3]	0.99788[−8]	0.94384[−8]	0.97361[−8]		0.49228[−3]
$^{131}_{54}$Xe	−2.7352[3]	0.22861[−7]	0.20836[−7]	0.22047[−7]		0.33255[−3]
$^{145}_{61}$Pm	−5.7936[3]	0.18088[−6]		0.15324[−6]		0.30374
$^{149}_{62}$Sm	−6.4288[3]	0.35220[−6]	0.18356[−6]	0.25042[−6]		0.22931[−1]
$^{151}_{63}$Eu	−7.1369[3]	0.15427[−5]	0.31767[−6]	0.56727[−6]	0.33[−6]	0.34753[1]
						(0.11071[1])
$^{155}_{64}$Gd	−7.9123[3]	−0.93326[−6]	0.85603[−6]	−0.36479[−4]	0.91[−6]	0.94663[2]
						(0.52931[−1])
$^{159}_{65}$Tb	−8.7684[3]	−0.41622[−6]		−0.52707[−6]		0.12444[1]
$^{175}_{71}$Lu	−1.6195[4]	−0.17641[−6]		−0.19130[−6]		0.17694
$^{193}_{77}$Ir	−2.9673[4]	−0.20660[−6]		−0.20689[−6]		0.17985[−2]
$^{229}_{90}$Th	−1.1064[5]	−0.70008[−5]	0.32846[−4]	−0.51283[−5]		0.13538[2]
$^{231}_{91}$Pa	−1.2262[5]	0.52550[−5]		0.11262[−4]		0.15633[4]
$^{235}_{92}$U	−1.3575[5]	0.18517[−5]	0.14965[−5]	0.15020[−5]		0.80784

[a)] For the calculations of the mixing coefficients the values of the $E\left(1s2s\ ^1S_0\right)$ and $E\left(1s2p\ ^3P_0\right)$ were used from Ref. [19].

Table 5. Off-diagonal hyperfine interaction matrix elements $\langle|h_{\rm hfs}|\rangle_2$ (in atomic unit a.u.) and mixing coefficients (a_2 and a_2') between the 1s2p ^{3}P$_0$ and 1s2p ^{1}P$_1$ states. For the calculations of a_2' the values of $E\left(1s2p\ ^3P_0\right)$ and $E\left(1s2p\ ^1P_1\right)$ were used from Refs. [19] and [20]. A is the 1s2s ^{1}S$_0$ $\rightarrow$ 1s^2 ^{1}S$_0$ transition rate in unit s^{-1} calculated including the 1s2p ^{3}P$_1$ and 1s2p ^{1}P$_1$ states.

Isotope	$\langle\|h_{\rm hfs}\|\rangle_2$	The mixing coefficients		A
		a_2	a_2'	
$^{13}_{6}$C	2.8434[−6]	0.22113[−4]		0.74038[−17]
$^{19}_{9}$F	3.5348[−5]	0.15284[−3]	0.15341[−3][a)]	0.98688[−16][a)]
$^{29}_{14}$Si	−2.6400[−5]	−0.62824[−4]	−0.62788[−4]	0.51594[−15]
$^{47}_{22}$Ti	−7.6697[−5]	−0.87001[−4]	−0.86937[−4]	0.87039[−12]
$^{57}_{26}$Fe	1.7173[−5]	0.13411[−4]	0.13400[−4]	0.60210[−12]
$^{71}_{31}$Ga	4.4483[−4]	0.21480[−3]	0.21462[−3]	0.10923[−7]
$^{85}_{37}$Rb	2.4357[−4]	0.66409[−4]	−0.66357[−4]	0.19659[−6]
$^{97}_{42}$Mo	−1.7726[−4]	−0.30703[−4]	−0.30680[−4]	0.68307[−5]

[a)] For the calculations of the mixing coefficients the values of $E\left(1s2p\ ^3P_0\right)$ and $E\left(1s2p\ ^1P_1\right)$ were used from Ref. [19].

Table 6. Comparison among hyperfine-induced M1 ($A_{\rm (HIT)}$), weak- and hyperfine-induced E1 ($A_{\rm (WIT)}$) and 2E1 ($A_{\rm (HIT)}$) 1s2s ^{1}S$_0$ $\rightarrow$ 1s^2 ^{1}S$_0$ transition rates (in unit s^{-1}). For the calculations of the transition rates of the weak and hyperfine-induced E1 transitions we used transition energies from Refs. [19] and [20].

Isotope	$A_{\rm (HIT)}$ [6]	$A_{\rm (WIT)}$	$A_{\rm (HIT)}$ [25]
$^{13}_{6}$C	2.6534[−8]	0.74038[−17]	3.300[5]
$^{19}_{9}$F	1.0863[−4]	0.98688[−16]	5.029[6]
$^{29}_{14}$Si	2.4493[−4]	0.51594[−15]	8.685[7]
$^{47}_{22}$Ti	1.3010	0.87039[−12]	
$^{57}_{26}$Fe	3.8221[−1]	0.60210[−12]	
$^{71}_{31}$Ga	1.9926[3]	0.10923[−7]	
$^{85}_{37}$Rb	5.5705[3]	0.19659[−6]	
$^{97}_{42}$Mo	1.5643[4]	0.68307[−5]	
$^{103}_{45}$Rh	7.9312[4]	0.32719[−2]	1.154[11]
$^{117}_{50}$Sn	4.4904[5]	0.49228[−3]	2.164[11]
$^{131}_{54}$Xe	3.5483[5]	0.33255[−3]	3.415[11]
$^{145}_{61}$Pm	5.1405[7][a)]	0.30374	
$^{149}_{62}$Sm	1.8321[6][a)]	0.22931[−1]	
$^{151}_{63}$Eu	6.7643[7]	0.34753[1]	
$^{155}_{64}$Gd	5.5892[5][a)]	0.94664[2]	
$^{159}_{65}$Tb	1.4199[7][a)]	0.12444[1]	1.1013[12]
$^{175}_{71}$Lu	1.4508[8]	0.17694	
$^{193}_{77}$Ir	3.3463[6]	0.17985[−2]	
$^{229}_{90}$Th	1.7894[8][a)]	0.13538[2]	6.439[12]
$^{231}_{91}$Pa	4.7512[9][a)]	0.15633[4]	
$^{235}_{92}$U	1.5277[8][a)]	0.80784	7.265[12]

[a)] These transition rates were deduced via scaling in Z.[6]

However, results with more accurate values of the energies[20] differs from the ones in Ref. [4]. In this table we also display the values of the weak- and hyperfine-interaction-induced 1s2s ^{1}S$_0$ $\rightarrow$ 1s^2 ^{1}S$_0$ E1 transitions rates

$$A(1s2s\ ^1S_0 \rightarrow 1s^2\ ^1S_0) = \frac{2.02613\times10^{18}}{\lambda^3}(2F+1)\left\{\begin{array}{ccc} 0 & F & I \\ F & 1 & 1 \end{array}\right\}^2 a^2|b|^2 S_{\rm E1}. \quad (20)$$

The agreement between our values (in the brackets) for the $^{151}_{63}$Eu and $^{155}_{64}$Gd ions and other theories[4] 1.1979 and 6.21075[−2] respectively is very good, when the same energies as in Ref. [4] were used (see Table 4).

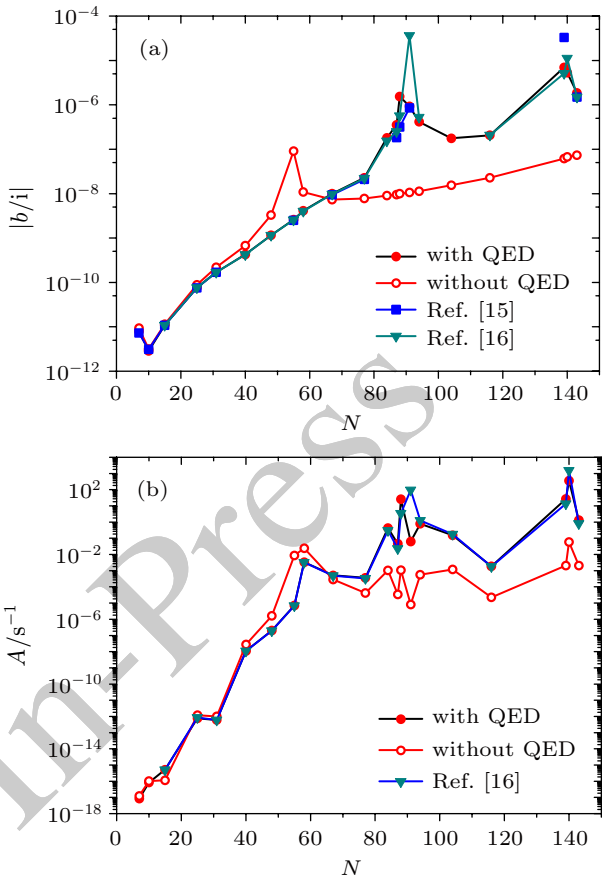

Fig. 2. Dependence of mixing coefficient $b/{\rm i}$ (absolute value) and transition rates A from number of neutrons (N).

Due to the strong hyperfine-induced mixing between the 1s2p ^{3}P$_0$ and 1s2p ^{1}P$_1$ states for the low-Z ions[18] we also included the 1s2p ^{1}P$_1$ state in the calculations. Here is given equation for mixing coefficients:

$$a_2 = \frac{\langle\Psi\left(1s2p\ ^1P_1F\right)|H_{\rm hfs}|\Psi\left(1s2p\ ^3P_0F\right)\rangle}{E\left(1s2p\ ^3P_0\right)-E\left(1s2p\ ^1P_1\right)}. \quad (21)$$

In Table 5 are given off-diagonal hyperfine interaction matrix elements $\langle|h_{\rm hfs}|\rangle_2$ (a.u.) and mixing coefficients (a_2) between the 1s2p ^{3}P$_0$ and 1s2p ^{1}P$_1$ states. For the $E\left(1s2p\ ^3P_0\right)$–$E\left(1s2p\ ^1P_1\right)$ transition energy QED effects are insignificant and the influence to the mixing coefficients a_2 is less than 0.9%. Comparing transition rate (A_1) (see Table 3) with A, it is clear that contributions of 1s2p ^{1}P$_1$ states are quite small (up to 3%).

Table 6 given E1 1s2s ^{1}S$_0$ $\rightarrow$ 1s^2 ^{1}S$_0$ transition rates ($A_{\rm (WIT)}$) arising from weak and off-diagonal hyperfine interactions. $A_{\rm (WIT)}$ are compared with transition rates of other 1s2s ^{1}S$_0$ $\rightarrow$ 1s^2 ^{1}S$_0$ decay channels: hyperfine-induced magnetic dipole transition rates M1 $A_{\rm (HIT)}$ and rates of two-photon electric dipole decay 2E1 ($A_{\rm (HIT)}$). Figure 2 reflects the importance of the QED effect to the $b/{\rm i}$ mixing coefficients and transition rates A. Filled circles show results computed with QED

and empty circles results without QED. Also there are results calculated using energies from Refs. [19] (square) and [20] (triangle). QED effects of order $(Z\alpha)^4$ for elements $^{151}_{63}$Eu, $^{155}_{64}$Gd, and $^{231}_{91}$Pa are important to the mixing coefficients of the weak interaction and transition rates A. Mixing coefficients b/i of weak interaction calculated without QED agree only in the beginning of the isoelectronic sequence ($Z = 6$, 9, 14, 22, and 26).

4. Conclusions

To sum up, we have calculated weak- and hyperfine-interaction-induced 1s2s ^{1}S$_0 \rightarrow$ 1s^2 ^{1}S$_0$ E1 transition rates for the isoelectronic sequence of He-like ions using the multiconfiguration Dirac–Hartree–Fock and relativistic configuration interaction methods. The comparison among our values and calculations of the transition rates of other 1s2s ^{1}S$_0 \rightarrow$ 1s^2 ^{1}S$_0$ decay channels are presented in Table 6. The calculated values differ from the previous calculations[4] for the $^{151}_{63}$Eu and $^{155}_{64}$Gd ions due to the importance of the high-order QED effects. Our results demonstrated that $^{151}_{63}$Eu, $^{155}_{64}$Gd, $^{229}_{90}$Th, and $^{231}_{91}$Pa He-like ions are the most promising for the future experiments due to the high values of the transition rates. We can also conclude that the present calculation method is able to describe correctly the weak interaction effects in highly charged ions.

Acknowledgment

The authors are thankful for the high performance computing resources provided by the Information Technology Open Access Center of Vilnius University.

References

[1] Khriplovich I B 1991 *Parity Nonconservation in Atomic Phenomena* (Philadelphia: Gordon and Breach)
[2] Ginges J S M and Flambaum V V 2004 *Phys. Rep.* **397** 63
[3] Gorshkov V G and Labzovskiĭ L I 1974 *JETP Lett.* **19** 394
[4] Labzowsky L N, Nefiodov A V, Plunien G, Soff G, Marrus R and Liesen D 2001 *Phys. Rev. A* **63** 054105
[5] Bondarevskaya A, Prozorov A, Labzowsky L, Plunien G, Liesen D and Bosch F 2009 *J. Phys.: Conf. Series* **163** 012012
[6] Li J G, Jönsson P, Gaigalas G and Dong C Z 2009 *Euro. Phys. J. D* **51** 313
[7] Rudzikas Z 2007 *Theoretical Atomic Spectroscopy*, 2nd edn. (Cambridge: Cambridge University Press)
[8] Grant I P 2007 *Relativistic Quantum Theory of Atoms and Molecules: Theory and Computation* (New York: Springer)
[9] Jönsson P, He X, Froese Fischer C and Grant I P 2007 *Comput. Phys. Commun.* **177** 597
[10] Jönsson P, Gaigalas G, Bieroń J, Froese Fischer C and Grant I P 2013 *Comput. Phys. Commun.* **184** 2197
[11] Gaigalas G, Rudzikas Z and Fischer Froese C 1997 *J. Phys. B: At. Mol. Opt. Phys.* **30** 3747
[12] Gaigalas G, Žalandauskas T and Rudzikas Z 2003 *At. Data Nucl. Data Tables* **84** 99
[13] Gaigalas G, Žalandauskas T and Fritzsche S 2004 *Comput. Phys. Commun.* **157** 239
[14] Jönsson P, Parpia F A and Froese Fischer C 1996 *Comput. Phys. Commun.* **96** 301
[15] Caso C, Conforto G, Gurtu A, *et al.*, (Particle Data Group) 1998 *Eur. Phys. J. C* **3** 1
[16] Berestetskii V, Lifshitz E and Pitaevskii L 1982 *Quantum Electrodynamics* (Oxford U.K., New York: Pergamon Press)
[17] Cowan R D 1981 *The Theory of Atomic Structure and Spectra* (Berkeley: University of California Press)
[18] Johnson W R, Cheng K T and Plante D R 1997 *Phys. Rev. A* **55** 2728
[19] Plante D R, Johnson W R and Sapirstein J 1994 *Phys. Rev. A* **49** 3519
[20] Artemyev A, Shabaev V, Yerokhin V, Plunien G and Soff G 2005 *Phys. Rev. A* **71** 062104
[21] Kramida A, Ralchenko Yu, Reader J and NIST ASD Team 2013 NIST Atomic Spectra Database (ver. 5.1) [online]. Available: `http://physics.nist.gov/asd3` [2014, May 29] National Institute of Standards and Technology, Gaithersburg, MD
[22] Johnson W R, Plante D R and Sapirstein J 1995 *Ad. At., Mol. Opt. Phys.* **35** 255
[23] Maul M, Schäfer A, Greiner W and Indelicato P 1996 *Phys. Rev. A* **53** 3915
[24] Brage T, Judge, P G, Aboussaïd A, Godefroid M R, Jönsson P, Ynnerman A, Froese Fischer C and Leckrone D S 1998 *Astrophys. J.* **500** 507
[25] Derevianko A and Johnson W R 1997 *Phys. Rev. A* **56** 1288